FORESTRY AGRICULTURE

International Journal
Sustainable Future for Human Security
J-SustaiN Vol. 3, No. 1 (2015) 25-31
http://www.j-sustain.com

Estimation of Canopy Resistance and Surface Moisture Availability in a Rice Paddy Field

Yanyan WANG[a], Hiroki OUE[b*]

[a]The United Graduate School of Agricultural Sciences, Ehime University. 3-5-7 Tarumi, Matsuyama, Ehime, Japan
[b]Faculty of Agriculture, Ehime University. 3-5-7 Tarumi, Matsuyama, Ehime, Japan

Received: April 14, 2015/ Accepted: April 24, 2015

Abstract

A surface moisture availability model (β model) parameterized by solar radiation *St*, soil water content θ and wind speed *u*, and a canopy resistance model (r_c model) parameterized by *St* under four different vapour pressure deficit VPD conditions were developed in this paper. β model showed that under larger *St*, higher θ and higher *u* conditions, β was larger. Under higher *St*, r_c was influenced by VPD more, and it meant stomatal aperture became sensible to VPD. When Bowen ratio *Bo* was zero, r_c was set as critical canopy resistance r_{cc}, and r_c-r_{cc} accounted for the energy partitioning directly.

Keywords: *Surface moisture availability; Canopy resistance; Solar radiation; Vapour pressure deficit; Soil water content.*

1. Introduction

Evapotranspiration is one of the main processes in the air-land energy exchanges. The evapotranspiration is controlled by atmospheric conditions, surface soil wetness and vegetational conditions. Quantification of soil evaporation can help in environment and irrigation management (Guo *et al*. [1]). The meteorological and vegetational factors have influence on the crop's energy budget (Oue [2]).

Many previous studies have parameterized surface moisture availability for bare-soil evaporation, making use of an empirical relationship between theevaporation rate and water content of the surface soil layer having a thickness of few centimetres (Mahfouf and Noihan [3]; Yamanaka *et al*. [4]). However, the soil water content is not steady under different solar radiation and wind speed conditions, so the relationships obtained under specific soil water condition are not applicable. In addition, the thickness of the soil layer used in determining the surface-moisture availability cannot be clearly defined (Yamanaka *et al*. [4]).

The measured surface moisture availability βis obtained by sensible heat flux, latent heat flux, relative humidity and air temperature. In this study, a simple model is developed for estimating surface moisture availability with solar radiation, soil water content at 5 cm and wind speed.

Canopy resistance is related to soil moisture, available energy, vapour pressure deficit and aerodynamic resistance (Gharsallah *et al*. [5]). According to Monteith [6], water vapour loss from a leaf by diffusion is equivalent to an electrical circuit with cuticular resistances being analogous to resistance to current flow. A number of empirical approaches have been proposed to estimate canopy resistance (Weert and Kamerling [7]; Slabbers [8]; Lafleur and Rouse [9]; Allen *et al* .[10]; Kim and Verma [11]; Saugier and Katerji [12]; Steiner *et al*. [13]; Lafleur and Roulet [14]; Todorovic [15]; Oue [2]; Katerji and Rana [16]; Abtew and Melsse [17]). In this study, the canopy resistance estimated with solar radiation is applied to show the stomatal response to the environment.

2. Field observations

Field observations were conducted from July 13th to November 18th, 2013 in the paddy field located in the Faculty of Agriculture, Ehime University, Matsuyama, Japan (33°50′ N, 132°47′ E). The schematic arrangement of observation site and its surroundings in Ehime University is shown in Fig. 1.

The experimental plot was 742.34 m², surrounded by greenhouses, orchards and upland fields. The fetch of it in the prevailing wind direction was 20.0 m. The black rice （*Oryzasativa* L.）was transplanted on July 1st with 30×20 cm spacing and it was harvested on November 18th, 2013.

The global solar radiation (*St*), albedo(α)and downward longwave radiation (*Ld*), and upward long wave radiation (*Lu*) were observed by CNR-2(Kipp & Zonen, Netherland) at 2.0 m. Air temperature and relative humidity were measured by the psychrometers HMP-45A (Vaisala, Finland). At first, two thermometers and hygrometers were set at 0.6m and 1.0 m, and with the growth of rice, sensors were lifted to 1.0 m and 1.5m, respectively on November 10th, 2013. Horizontal wind speed was observed above the canopy by the three-cup anemometer 014A (Met One, USA) mounted at 0.6m, 1.0 m and 2.0 m initially. For the same reason, the two lower anemometers were lifted to 1.0 m and 1.5m on November 10th, 2013. Soil temperature, soil heat flux and water content were measured by TE-5 (Decagon, USA)

* *Corresponding Author: Hiroki OUE*
Tel.: +81899469887;Fax.: +81899469887;E-mail: oue@agr.ehime-u.ac.jp

at the soil depth of 0, 5cm, 10cm and 20cmin the paddy field. All data were sampled 10s, and recorded every 10 min by a data logger CR23x (Campbell, USA).

Water depth and plant height were measured twice (8:00 and 18:00) every day, while leaf area index LAI was measured with five plants once a week.

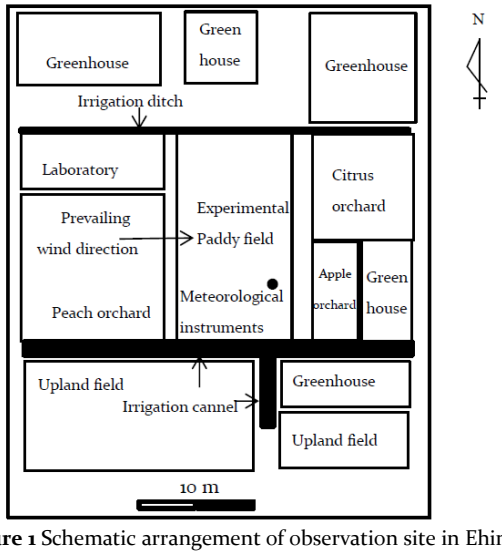

Figure 1 Schematic arrangement of observation site in Ehime University in 2013

3. Material and method

Net radiation *Rn* is written as eq. (1).

$$Rn = (1-\alpha)St + Ld - Lu \quad (1)$$

Energy balance in a paddy field is written as eq. (2).

$$Rn = H + LE + G + \delta W \quad (2)$$

$$\delta W = C_w d_w \frac{T_{w(t+1)} - T_{w(t)}}{\delta t} \quad (3)$$

where H is sensible heat flux (W m^{-2}), LE is latent heat flux (W m^{-2}) and δW is the timely change of energy storage per unit area of water (W m^{-2}). In eq. (3), C_w is the specific heat capacity of water (4.18 J cm^{-3} K^{-1}), d_w is the water depth (cm), T_w is water temperature (K), and δt is time period (s).

H and LE can be estimated by Bowen ratio energy budget method.

$$Bo = \gamma(T_1 - T_2)/(e_1 - e_2) \quad (4)$$

$$LE = (Rn - G - \delta W)/(1 + Bo) \quad (5)$$

$$H = C_p \rho C_h u (T_s - T_a) \quad (6)$$

$$LE = C_p \rho C_h u \beta (e_{sat}(T_s) - e_a)/\gamma \quad (7)$$

where Bo is Bowen ratio, γis psychrometric constant (0.66 hPa K^{-1}), C_h is bulk transfer coefficient, u is wind speed at 2.0 m (m s^{-1}), T_s is surface temperature on the paddy field (℃), T_1 and T_2 are temperatures measured at two different heights (℃), e_1 and e_2 are vapour pressures at two heights corresponding to the temperature measurement (hPa), e_{sat} (T_s) is saturated vapour pressure at the surface temperature (hPa), e_a is air vapour pressure (hPa), β is surface moisture availability and ρ is air density (kg m^{-3}).

$$\rho = P / R_{specific} / T_a \quad (8)$$

Air density changes with variation of absolute pressure P (hPa) and air temperature T_a (eq. (8)). $R_{specific}$ is the specific gas constant (287.058 J kg^{-1} K^{-1}).

Actual evapotranspiration ET is estimated from LE of eq. (5) as shown in eq. (9).

$$ET = LE \times 3.6/l \quad (9)$$

where l is latent heat of vapour.

4. Results and discussion

4.1 Plant height (h) and LAI

Plant height (h) and LAI of black rice measured from July 1st to November 18th are shown in Fig. 2. On transplanting day, h was 13.0 cm, and LAI was 0.02. Before it was harvested, h was 103.0 cm, and LAI was 5.4. The flowering days were September 5th to 9th, 2013.

Based on observations in the paddy field, the total growth period could be divided into four stages: (1) last stage of tiller, (2) early stage of reproductive growth phase, (3) booting and flowering stage, (4) ripening stage. From stage 1 to 3, h and LAI increased greatly, and the largest LAI was 6.7 on September 25th.

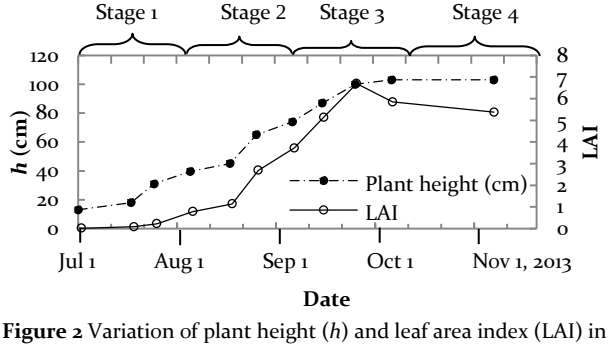

Figure 2 Variation of plant height (h) and leaf area index (LAI) in the paddy field from July 1 to Nov 18, 2013

4.2. Rainfall and soil water content at 5 cm

Rainfall was 182.0 mm in August, and 156.0 mm in September, 2013.

As shown in Fig. 3, from stage 1 to 3, soil water content (θ) at 5 cm was averagely 47.0 % due to the intermittent irrigation and rainfall. In stage 4, without irrigation water, θ was low mostly. Only on October 24th and 25th, it was high, and that's because of the storm from October 23rdto 24th, 2013.

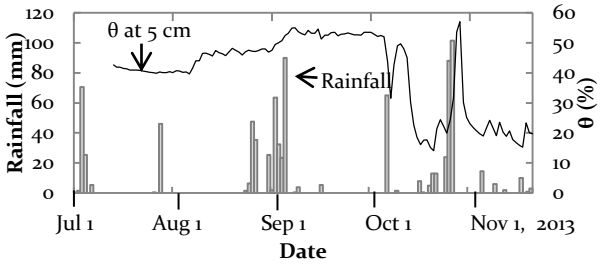

Figure 3 Rainfall from July 1 to Nov 18 and soil water content (θ) at 5 cm from July 13 to Nov 18, 2013

4.3. Actual evapotranspiration *ET* and evapotranspiration ratio *K*

The actual evapotranspiration *ET* calculated by Bowen ratio energy balance method (eq. (4) and (5)) and evapotranspiration ratio *K* are shown in Fig. 4. And *K* was obtained by *ET* dividing Penman's potential evaporation *EP*.

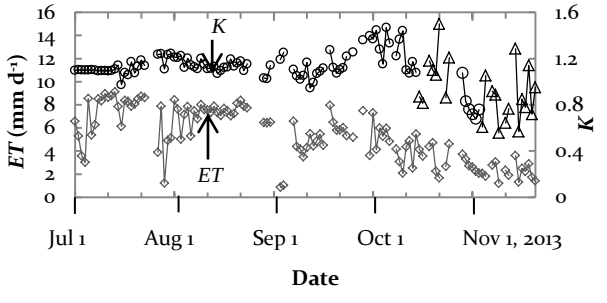

Figure 4 Evapotranspiration *ET* (◇) and evapotranspiration ratio *K* (○; wet conditions and △; dry conditions)

From stage 1 and 2, *K* was averagely 1.12 mainly because LAI in the irrigated field was less than 3.8. Based on the *K* in stage 1 and 2, the *K* model was developed with *St*, because *St* had highest correlation with *K* (as eq. (10)).

$$K = -0.0005St^2 + 0.0015St + 1.091 \quad (10)$$

Before starting the experiment, *ET* from July 1st to 12th was calculated by averaged *K* from stage 1 to 2 and multiplied by *EP*, which was calculated with data at Japan Meteorological Agency in Matsuyama.

In stage 3, averaged *K* increased to 1.18 because LAI increased, and the largest *K* was 1.43. LAI had priority influence on *K*, and the relationship between LAI and *K* is as shown in eq. (11).

$$K = 0.0734\mathrm{LAI}^2 - 0.7439\mathrm{LAI} + 2.8979 \quad (11)$$

In stage 4, *K* decreased to 0.97 because rice became ripe, and there was no irrigation water. There were two dry periods (the first one was from October 11th to 22th and the second one was from November 1st to 17th) and a wet period in stage 4. In the wet condition after rainfall, the averaged *K* was 1.15. Fig. 5 shows the relationship between soil water content θat 5 cm and *K* in these two dry periods. In the first and second dry period, the relationship could be written as eq. (12) and (13), respectively.

$$K = 1.0988\theta + 0.8671 \quad (12)$$

$$K = 1.9636\theta + 0.4569 \quad (13)$$

Because the plant became yellow, and *K* was lower in the second dry period than that in the first dry period, and it was concluded that *K* was influenced by growth stage instead of soil water content.

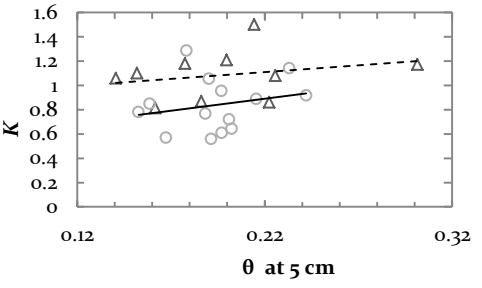

Figure 5 Relationships between soil water content (θ) at 5 cm and *K* in two dry periods in stage 4: (a) Oct 11-22 (△), (b) Nov 1-17 (○)

4.4. Energy budget

The diurnal variations of the energy budget terms in the four stages in the paddy field are shown in Fig. 6. In stage 1, *Rn* was large lyal located to latent heat flux *LE*. In the afternoon, *LE* was greater than *Rn* because of the negative sensible heat flux *H*. In stage 1 and 2, because the water in the paddy field stored quite amount of heat energy during daytime, so δ*W* was important. In the last two stages, *LE* was the main factor accounting for the energy budget compared with *H*, *G* and δ*W*. Based on the different soil water contents in stage 4, the energy budget analysis was divided into three situations: the first dry period, wet period and the second dry period, as shown in Fig. 6 (d_1), (d_2) and (d_3), respectively. In the two dry periods, *Rn* was less allocated to *LE*.

4.5. β model

The surface moisture availability β model was developed with solar radiation *St*, soil water content θ at 5 cm, wind speed *u* as shown in eq. (14).

$$\beta = \frac{a}{1/(St/100\times\theta)^2 - 0.05u} + b \quad (14)$$

where *a* and *b* are experiment parameters; *a* represents the surface moisture availability in response to the influencing factors classified by VPD.

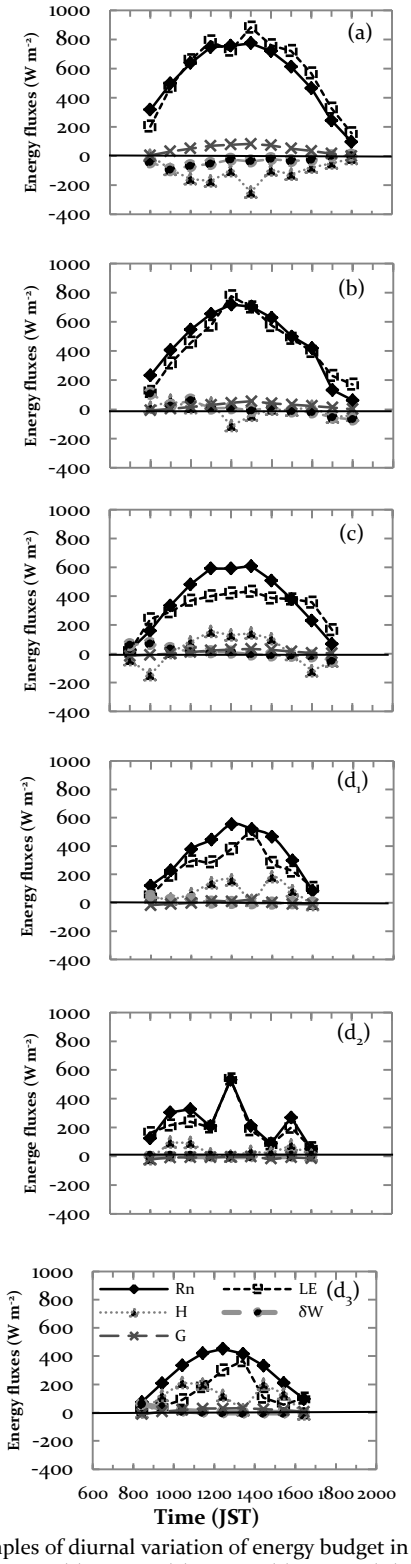

Figure 6 Examples of diurnal variation of energy budget in the paddy field in 4 stages: (a) July 24, (b) Aug 15, (c) Sep 24, (d_1) Oct 17 in the first dry condition of stage 4, (d_2) Oct 26 in wet condition of stage 4, (d_3) Nov 1 in the second dry condition of stage 4

Relationships between *St*, θ and *u* and surface moisture availabilityβ classified by four ranges of VPD are shown in Fig. (7).

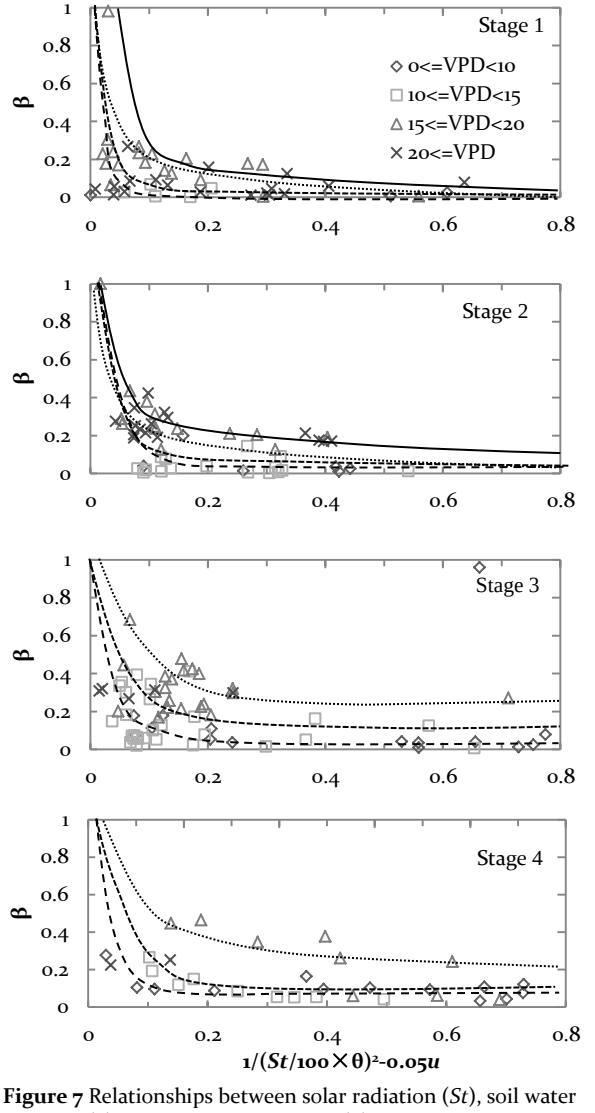

Figure 7 Relationships between solar radiation (*St*), soil water content (θ) at 5 cm and wind speed (*u*) and surface moisture availability (β)classified by four ranges of vapour pressure deficit (VPD)

4.6. r_c model

Theoretical and empirical approaches have been applied to show that canopy resistance r_c is related to θ, vapour pressure deficit VPD and aerodynamic resistance r_a (Gharsallah *et al.* [5]). The r_a has been commonly presented mainly as a function of surface characteristics and wind speed *u* (Abtew W and Melesse A [18]). r_c can be estimated from *LE*, as shown in eq. (15).

$$r_c = \frac{C_p \rho (e_{sat}(T_s) - e_a}{\gamma LE} - r_a \qquad (15)$$

$$r_a = \frac{\{\ln[(z-d)/z_0] - \psi_m\}\{\ln[(z-d)/z_{0v}] - \psi_v\}}{k^2 u} \qquad (16)$$

In eq. (15) and eq. (16), z is the height of wind measurement (m), d is displacement height (=0.667 h), z_o is the roughness length for momentum transfer (=0.123 h), z_{ov} is the roughness length for vapour (=0.0123 h), k is the von Karman constant forturbulent diffusion (0.41), and u is wind speed measurement at height z (ms^{-1}). Ψ_m and Ψ_v are the Monin-Obukhov similarity functions for momentum and water vapor transfer (Brutsaert [19]) shown as follows.

$$\text{If } (z\text{-}d)/L \geq o \qquad \begin{aligned} \Psi_m &= -5(z-d-z_0)/L \\ \Psi_v &= -5(z-d-z_{0v})/L \end{aligned} \qquad (17)$$

$$\text{If}(z\text{-}d)/L < o \qquad \Psi_m = \ln\frac{(1+x^2)(1+x)^2}{(1+x_0^2)(1+x_0)^2} - 2\left[\tan^{-1}(x) - \tan^{-1}(x_0)\right]$$

$$\Psi_v = 2\ln\frac{(1+x^2)}{(1+x_{0v}^2)} \qquad (18)$$

$$\begin{aligned} x &= [1-16(z-d)/L]^{\frac{1}{4}} \\ x_0 &= (1-16z_0/L)^{\frac{1}{4}} \\ x_{0v} &= (1-16z_{0v}/L)^{\frac{1}{4}} \end{aligned} \qquad (19)$$

where L is Obukhov's stability length.

Environmental factors affecting stomatal conductance include St, T_a, e_a and leaf water status. The most consistent and well-documented stomatal response is the opening that occurs in most species as St increases, and stomata tend to open as T_a increases over the normally encountered range, and the stomata in many species close in response to increased leaf-to-VPD difference, and stomata tends to close with increasing leaf water potential (Hamlyn G. Jones [20]).

Based on the measured results, Oue [2] revealed St had the primary influence on r_c and VPD had second influence on r_c. And Oue [2] developed a simple model to estimate r_c with St classified by four ranges of VPD (as eq. (20)).

$$r_c = m/St + n \qquad (20)$$

where m and n are experimental parameters; m represents the canopy resistance r_c in response to the solar radiation St.

The relationships between St and r_c classified by four ranges of VPD are shown in Fig. 8. In the four stages, the variation trends of r_c were similar as a whole, with the increase of St, r_c decreased fast at first, and after that it tended to be steady.

Combining eq. (7) and (9), actual evapotranspiration ET can be estimated by r_a and r_c as shown in eq. (21).

$$ET = C_p \rho C_h \frac{r_a}{r_a + r_c}\left[e_{sat}(T_s) - e_a\right] \times 3.6/\gamma/l \qquad (21)$$

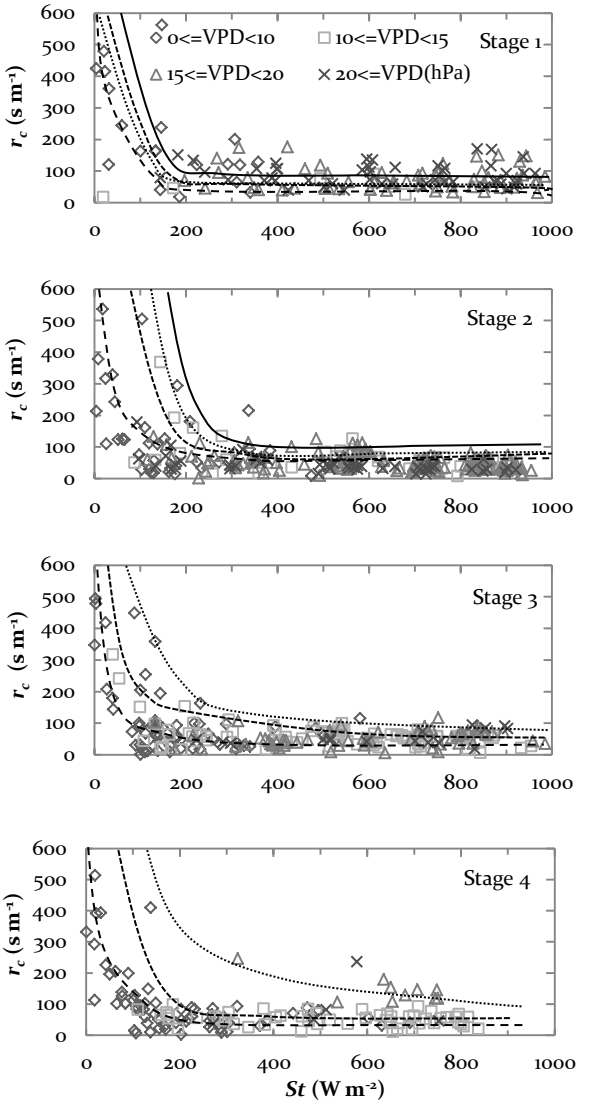

Figure 8 Relationships between solar radiation (St) and canopy resistance (r_c) classified by four ranges of VPD

4.7. Parameterization of β model and r_c model

Since the relationship between St, θ and u and surface moisture availability βwere classified by four ranges of VPD, and there were four groups of parameters in every model.

As shown in Fig. 9, a increased with the increase of VPD in each stage. It meant under higher VPD condition, β was sensitive to St, θ and u.

In r_c model, under higher VPD condition, m was higher in each stage. It meant under larger St, r_c was influenced by VPD more, and the stomatal aperture became sensitive to VPD.

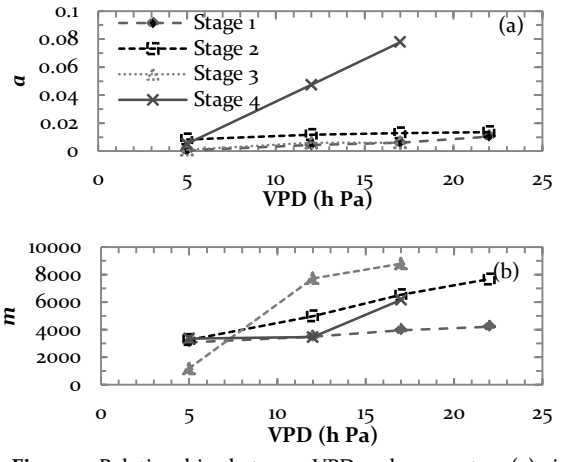

Figure 9 Relationships between VPD and parameters (a) *a* in βmodel and (b) *m* in r_c model

4.8. Modelled actual evapotranspiration *ET*

Comparison of measured *ET* by Bowen ratio energy balance method and modelled *ET* by β model and r_c model are shown in Fig. 10. T-test: paired two samples for means showed that the modelled *ET* and measured *ET* were highly corresponded at the 95 % level.

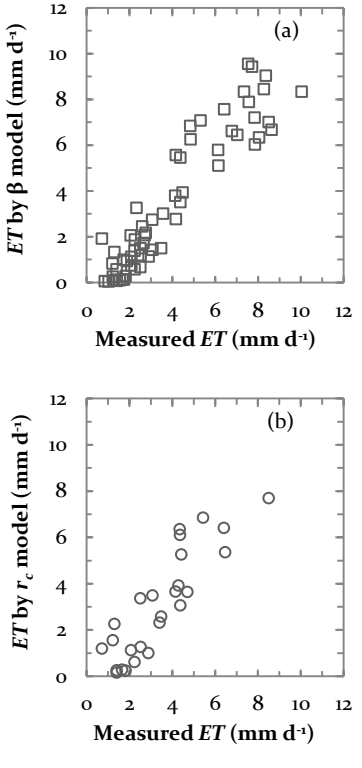

Figure 10 Comparison of measured and modelled *ET* (a) by β model and (b) by r_c model

4.9. Relationship between r_c and Bowen ratio *Bo*

Relationship between canopy resistance r_c and Bowen ratio *Bo* classified by four growing stages are shown in Fig. 11. In each stage, there was no clear relationship between canopy resistance r_c and *Bo* (correlation coefficient was less than 0.01). Therefore, we concluded r_c did not account for energy partitioning directly.

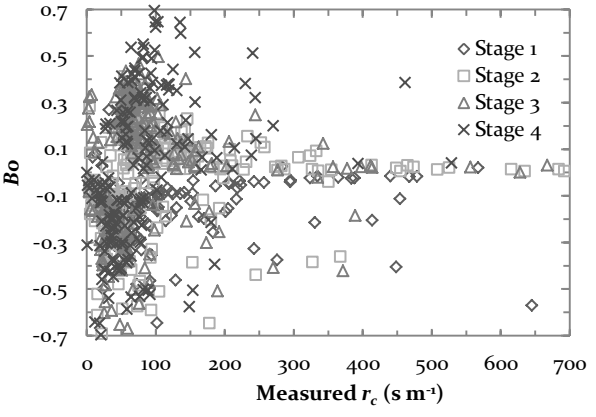

Figure 11 Relationship between canopy resistance (r_c) and Bowen ratio (*Bo*) classified by four stages

4.10. Relationship between critical canopy resistance r_{cc} and Bowen ratio *Bo*

Critical canopy resistance r_{cc} was defined as r_c when *Bo* was zero. The relationship between *St* and r_{cc} classified by four ranges of VPD showed that with the increase of *St*, r_{cc} decreased (Fig. 12).

The difference between canopy resistance and critical canopy resistance r_c-r_{cc} had the linear relationship with *Bo* in each stage (Fig. 13). So it was r_c-r_{cc} that accounted for the energy partitioning directly.

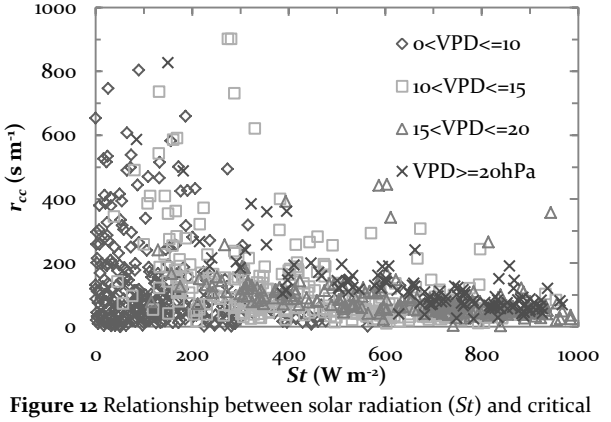

Figure 12 Relationship between solar radiation (*St*) and critical canopy resistance (r_{cc}) classified by four ranges of VPD

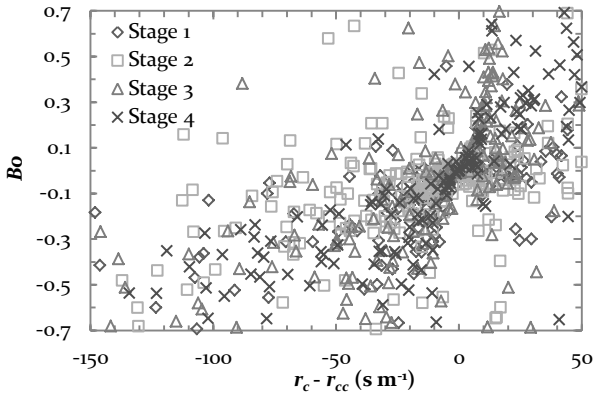

Figure 13 Relationships between (r_c-r_{cc}) and Bowen ratio (*Bo*) classified by four stages

5. Conclusions

The influence of meteorological and vegetational factors on the partitioning of the energy of a rice paddy field was evaluated in this study.

The surface moisture availability model showed that under larger solar radiation *St*, higher soil water content θ and higher wind speed *u* conditions, the surface moisture availabilityβwas larger.

For canopy resistance r_c, under higher *St*, r_c was influenced by VPD more, and it meant stomatal aperture became sensible to VPD.

Since there was no clear relationship between canopy resistance r_c and Bowen ratio *Bo*, so we concluded that r_c did not account for the energy partitioning directly.

When *Bo* was zero, the canopy resistance r_c was set as critical canopy resistance r_{cc}. And r_c-r_{cc} had the linear relationship with *Bo* in each stage. It meant that r_c-r_{cc} accounted for the energy partitioning directly.

Acknowledgements

Thanks Professor H. Sugimoto in the Crop Science laboratory, Faculty of Agriculture, Ehime University for supporting our measurements in the paddy field.

References

[1] Guo YQ, Ben-Asher J, Yano T, Momii K. Estimation of soil evaporation using the differential temperature method. *Soil Science* 1999;**63**(6):1608-1614.

[2] Oue H. Influence of meteorological and vegetational factors on the partitioning of the energy of a rice paddy field. *Hydrolprocess* 2005;**19**:1567-1583.

[3] Mahfouf JF, Noihan J. Comparative study of various formulations of evaporation from bare soil using in situ data. *J Appl. Meteorol* 1991;**30**:1354-1365.

[4] Yamanaka T, Takeda A, Sugita F. A modified surface-resistance approach for representing bare-soil evaporation: wind tunnel experiments under various atmospheric conditions. *Water Resour Res* 1997;**33**(9):2117-2128.

[5] Gharsallah O, Moncini M, Rana G. Bulk canopy resistance: determination and modelling for actual evapotranspiration estimation of maize. *IX Convegno Nazionale dell' Associazione Its lisns di Ingegneria Agraria*, Ischia Porto; 2009.

[6] Monteith JL. *Principles of environmental physics*. Edward Arnold, London, UK; 1973.

[7] Weert RVD, Kamerling GE, Evapotranspiration of water hyacinth (Eichhornia crassipes). *J Hydrol* 1974;**22**:201-212.

[8] Slabbers PJ. Surface roughness of crops and potential evapotranspiration. *J Hydrol* 1977;**34**:181-191.

[9] Lafleur PM, Rouse WR. The influence of surface cover and climate on energy partitioning and evaporation in subarctic wetland, *Bound Layer Meteorol* 1988;**44**:327-329.

[10] Allen RG, Jensen ME, Wright JL, Burman RD. Operational estimation of reference evapotranspiration. *Agron*1989;**81**:650-662.

[11] Kim J, Verma SB. Modeling canopy stomatal conductance in a temperate grassland ecosystem. *Agric Forest Meteorol* 1991;**55**:149-166.

[12] Saugier B, Katerji N. Some plant factors controlling evapotranspiration. *Agric Forest Meteorol* 1991;**54**:263-277.

[13] Steiner JL, Howell TA, Schneider AD. Lysimetric evaluation of daily potential evapotranspiration models for grain sorghum. *Agron*1991;**83**:240-247.

[14] Lafleur PM, Roulet NT. A comparison of evapotranspiration rates from two fens of the Hudson Bay Lowland. *Aquat Bot* 1992;**44**:59-69.

[15] Todorovic M. Single-layer evapotranspiration model with variable canopy resistance. *J Irrigation and Drain Eng* 1999;**125**(5):235-245.

[16] Katerji N, Rana G. *Crop evapotranspiration measurement and estimation in the Mediterranean region*. INRA-CRA, Bari; 2008.

[17] Wossenu Abtew, Assefa Melesse. *Evaporation and evapotranspiration*. Springer Dordrecht Heidelberg, UK; 2013.

[18] Abtew W, Gregory JM, Borrelli J. Wind profile: estimation of displacement height and aerodynamic roughness. *Trans ASAE* 1989;**38**(1):121-129.

[19] BrutsaertnW. *In Evaporation into the Atmosphere.* Kluwer Academic: Dordrecht; 1982.

[20] Hamlyn G. Jones. *Plants and microclimate: a quantitative approach to environmental plant physiology*. 3rd ed. Cambridge, UK; 2014.